Impact ionization rate in ZnS

Martin Reigrotzki, Michael Stobbe, and Ronald Redmer
Universität Rostock, Fachbereich Physik, Universitätsplatz 3, D-18051 Rostock, Germany

Wolfgang Schattke
Institut für Theoretische Physik, Christian-Albrechts-Universität Kiel, Leibnizstraße 15, D-24118 Kiel, Germany
(Received 14 February 1995)

The impact ionization rate and its orientation dependence in **k** space are calculated for ZnS. The numerical results indicate a strong correlation to the band structure. The use of a q-dependent screening function for the Coulomb interaction between conduction and valence electrons is found to be essential. A simple fit formula is presented for easy calculation of the energy-dependent transition rate.

The impact ionization rate is of basic interest in understanding the electron transport in semiconductors at high-electric-field strengths. This microscopic quantity is necessary for calculating the probability of the electron to ionize, which is described by the ionization coefficient α. Interesting features are the orientation dependence and the threshold behavior, which were studied for Si (Refs. 1–4) and GaAs.[3,5]

Recently, we have determined the ionization rate for GaAs and Si,[3] following a scheme presented by Sano and Yoshii[2] for the evaluation of the impact ionization rate for Si using a very efficient deterministic numerical procedure. Their special integration scheme takes into account a rather high number of points in the Brillouin zone, so that they were able to study effects of the anisotropy in **k** space as well as the threshold behavior for Si. Both were found to be direct consequences of the band structure.

In this paper we investigate the impact ionization rate and its orientation dependence in the wide-band-gap semiconductor ZnS ($E_G = 3.63$ eV). The calculation is performed similar to Ref. 3, utilizing the integration method of Sano and Yoshii[2] again.

Inserting a band structure which is obtained from local pseudopotential parameters for ZnS, the correlation of the particular band shapes with the impact ionization rate is shown. Exchange and umklapp processes are included in the evaluation of the impact ionization rate. The consideration of an appropriate wave-vector-dependent screening function for the Coulomb interaction in semiconductors is of significant influence on the results.

The impact ionization rate is usually determined from Fermi's golden rule,

$$r(\mathbf{k}_1,\nu_1) = \frac{2\pi}{\hbar}\frac{\Omega^3}{(2\pi)^9}\sum_{\nu_2\cdots\nu_4}\int\cdots\int d^3k_2 d^3k_3 d^3k_4\,|M_{\rm tot}(1,2;3,4)|^2\,\delta\left[E_{\nu_1}(\mathbf{k}_1)+E_{\nu_2}(\mathbf{k}_2)-E_{\nu_3}(\mathbf{k}_3)-E_{\nu_4}(\mathbf{k}_4)\right]\,, \quad (1)$$

where Ω and ν_i are the crystal volume and the band index, respectively, $M_{\rm tot}$ denotes the matrix element for ionization including direct (D), exchange (E), and umklapp processes,

$$|M_{\rm tot}|^2 = 2|M_D|^2 + 2|M_E|^2 - |M_D^* M_E + M_D M_E^*|\,. \quad (2)$$

The initial electron states belong to the conduction (1) and valence bands (2), whereas the final ones are both in the conduction band [(3) and (4)]. The integrals are extended over the Brillouin zone. The ionization rate, Eq. (1), is integrated over all directions in **k** space to get an averaged, only energy-dependent impact ionization rate,

$$R(E) = \frac{\sum_{\nu_1}\int d^3k_1\;\delta\left[E_{\nu_1}(\mathbf{k}_1)-E\right]\;r(\mathbf{k}_1,\nu_1)}{\sum_{\nu_1}\int d^3k_1\;\delta\left[E_{\nu_1}(\mathbf{k}_1)-E\right]}\,. \quad (3)$$

The analytical evaluation of the transition rate[6,7] requires strongly simplifying assumptions such as a parabolic band structure and free-electron wave functions, which are not well founded for semiconductors with a direct (GaAs, ZnS) or even an indirect gap (Si, ZnS when omitting the first conduction band which is not contributing). Therefore, we numerically evaluate Eqs. (1) and (3) in order to take into account a realistic band structure and corresponding wave functions in the entire Brillouin zone. This is done using a grid method following Sano and Yoshii,[2] who made extensive use of symmetry relations imposed by the crystal structure and were able to take into account a great number of points in the Brillouin zone for the evaluation of the integrations in Eq. (1) for Si. This method is accurate enough to treat even more sensitive effects such as the threshold behavior or the orientation dependence of the interband transition rate successfully.

We have calculated the band structure and wave functions within the frame of the empirical pseudopotential method,[8] utilizing the set of pseudopotential parameters from Ref. 9. The expansion runs over 113 **G** vectors to produce a reasonable band structure in the entire Brillouin zone and, especially, to give a realistic description

near the threshold. A plot of the band structure is presented in Fig. 1.

The interaction between the electrons in the bands is described by a statically screened Coulomb potential. The consideration of the wave-vector dependence of the dielectric function $\epsilon(q)$ is of importance for the calculation of the matrix elements in semiconductors as pointed out already by Laks *et al.*[10] For the interaction between conduction and valence electrons, we apply a q-dependent dielectric function derived by Levine and Louie.[11] This model incorporates the correct long-range and short-range properties of the dielectric function and, in addition, some consequences of the presence of a gap in the excitation spectrum as characteristic of semiconductors. The interaction between electrons in the conduction band can be modeled by a Debye potential with an inverse screening length $\kappa = [n_0 e^2/(\epsilon_0 k_B T)]^{-1/2}$ for a temperature of $T = 300$ K and a corresponding electron density of $n_0 = 10^{16}$ cm^{-3}. The choice of n_0 is of less importance, as there are very few ionization events with small momentum transfers of $q \approx \kappa$.

The $\mathbf{k}$ vectors are restricted to the first Brillouin zone with respect to the reduced zone scheme. We want to mention at this point that for umklapp processes we have to consider terms which go beyond the expansion up to the 113 $\mathbf{G}$ vectors of the pseudopotential band-structure calculation. The respective expansion coefficients, i.e., those belonging to reciprocal lattice vectors with $|\mathbf{G}| > \sqrt{20}(2\pi/a)$, were calculated by means of perturbation theory.[3,12]

For the numerical treatment of Eqs. (1) and (3) the δ function is replaced here by rectangles of unit area with a height of $1/\delta E$ and a corresponding width of δE. A value of $\delta E = 0.1$ eV was found to be large enough to ensure good convergence. This was proved by test calculations with a finer grid as well as with a value of $\delta E = 0.2$ eV. Of course, the broadening factor is related to effects such as collision broadening and intracollisional field effects.[13] However, the study of such effects is not intended here.

An important feature of the grid method used in our previous paper[3] and in Ref. 2 is that the storage of energy values and wave functions can be restricted to the irreducible wedge (IW) if the symmetry properties of the Brillouin zone are fully exploited. The wave function for a wave vector $T_{\mathbf{k}}\mathbf{k}$, which is obtained by operating one of the 48 transformations $T_{\mathbf{k}}$ of the lattice point group on a wave vector $\mathbf{k}$ of the IW, is then determined from $\alpha^{\nu}_{\mathbf{G}}(\mathbf{k})$ (see Refs. 2 and 3). The mesh in $\mathbf{k}$ space is constructed with regard to the limits of the IW,

$$0 \le k_x + k_y + k_z \le 1.5\left(\frac{2\pi}{a}\right),$$

$$0 \le k_z \le k_y \le k_x \le \left(\frac{2\pi}{a}\right),$$

as well as to the condition for the interval length of the assumed grid $\Delta k_i = (1/n)(2\pi/a)$, $i = \{x, y, z\}$ with $n \in \aleph$.

For the determination of the ionization rate $r(\mathbf{k}, \nu)$, we take a mesh of 152 points in the IW [$\Delta k_i = \frac{1}{10}(2\pi/a)$]. For the study of the average ionization rate $\bar{R}(E)$, the summations over the conduction-band indices were restricted to the four lowest bands, whereas all four valence bands were taken into account.

In order to investigate the influence of the band structure (see Fig. 1) on the ionization rate, we examine $r(\mathbf{k}_1, \nu_1)$ [Eq. (1)], especially along three symmetry lines. In the first conduction band there are no points at all satisfying the threshold condition and, therefore, the total rate is due to electrons in the higher—mainly the third and fourth—conduction bands. The anisotropy of the ionization rate of ZnS for electrons initiating from the second, third, and fourth bands is shown in Fig. 2. Comparing these results with the band-structure data, a coincidence of the qualitative behavior of the impact ionization rate for the three directions and the third and fourth conduction bands can be stated. However, the attempt to manifest this correlation by applying a power-law fit formula for $r(\mathbf{k}_1, \nu_1)$ as used in our prevoius paper[3] did not lead to a satisfactory result. The validity of this Keldysh-type fit[14] strongly relies on the isotropy of the matrix elements. Contrary to calculations for GaAs (Ref. 3) and Si,[2,3] these exhibit a notable dependence on the $\mathbf{k}$

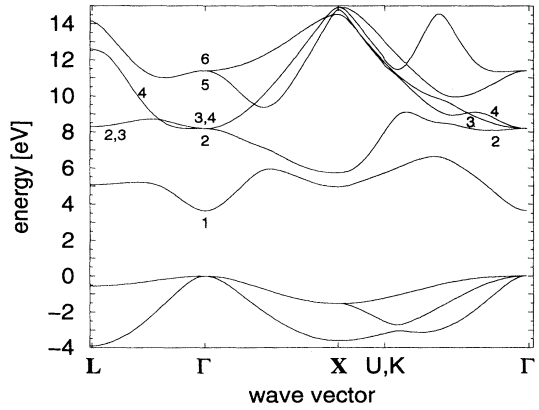

FIG. 1. Pseudopotential band structure of ZnS. The labels indicate the conduction bands including degeneracies.

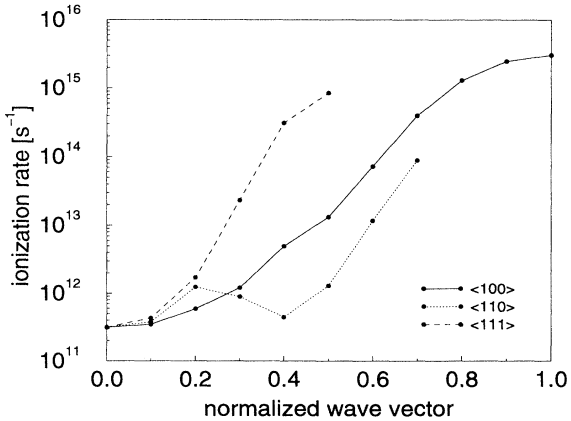

FIG. 2. Ionization rate for ZnS calculated for $\mathbf{k}$ points along three symmetry lines.

value of the initial electron, which hence does not allow for such a fit.

Furthermore, the necessity to consider the region of enlarged energies above the second conduction band, where band degeneracies and multiple level crossings occur, complicates the correlation of impact ionization to the band structure. For such high energies, also the quality of empirical pseudopotential band structures becomes questionable. The desirable application of a nonlocal band structure may lead to more rigorous results for the impact ionization rate.

The average energy-dependent ionization rate $R(E)$ can, however, be approximated by such a simple fit formula, which is given by

$$\tilde{R}(E) = P[E - E_{\mathrm{th}}]^a \quad , \tag{4}$$

where the parameters are fixed to $P = 5.14 \times 10^{10}$ $\mathrm{s}^{-1}\,(\mathrm{eV})^{-a}$ and $a = 5.183$. The threshold energy was set to $E_{\mathrm{th}} = 3.8$ eV (the calculation gave first ionization events above $E_{\mathrm{th}} = 3.93$ eV; regarding E_{th} as a fit parameter, best fits may be obtained with $E_{\mathrm{th}} \approx 3.5$ eV). Figure 3 shows the result as obtained from our numerical calculations together with the fit $\tilde{R}(E)$. The increase of the curve indicates a threshold behavior similar to that obtained for GaAs, a typical wide-band-gap semiconductor with a hard threshold.

We have neglected in our present calculations phonon-assisted impact ionization processes as well as deep-level ionization, which may become of importance at high fields. Furthermore, other high-field effects, such as collision broadening or the intracollisional field effect, have to be considered for a more comprehensive description of the transport process of hot electrons in semiconductors similar to Refs. 13 and 15.

The aim of further calculations may be the study of the influence of the obtained anisotropy effects on the ionization coefficient, where an additional effect of the band structure is expected.[16] Furthermore, the influence of dynamic screening, which was found to be substantial for Si,[17] has to be studied also for ZnS. The inclusion of the obtained impact ionization rate would also improve present calculations for high-field transport in ZnS.[18,19]

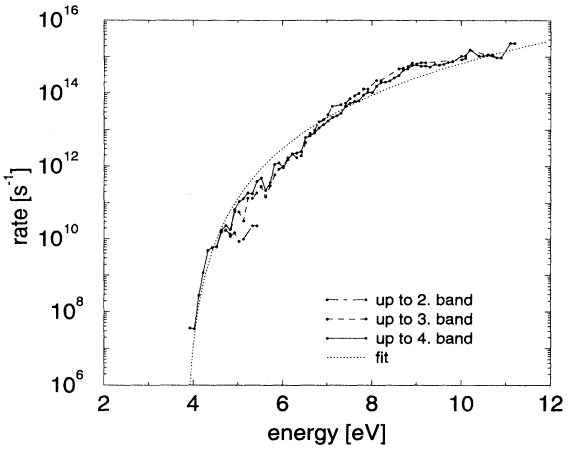

FIG. 3. Average ionization rate for ZnS obtained from the present numerical calculation and from the fit formula [Eq. 4], indicating the contributions of the lowest four conduction bands.

We would like to thank Steve Goodnick and Shankar Pennathur for helpful comments. This work was supported by the Deutsche Forschungsgemeinschaft under Grants Nos. Re 882/6-1 and Sha 360/8-1.

[1] J. Bude and K. Hess, J. Appl. Phys. **72**, 3554 (1992).
[2] N. Sano and A. Yoshii, Phys. Rev. B **45**, 4171 (1992).
[3] M. Stobbe, R. Redmer, and W. Schattke, Phys. Rev. B **49**, 4494 (1994).
[4] N. Sano and A. Yoshii, J. Appl. Phys. **75**, 5102 (1994).
[5] Y. Wang and K. Brennan, J. Appl. Phys. **71**, 2736 (1992).
[6] The analytical approaches are reviewed by D. J. Robbins, Phys. Status Solidi B **97**, 9 (1980); **97**, 387 (1980); **98**, 11 (1980).
[7] W. Quade, E. Schöll, F. Rossi, and C. Jacoboni, Phys. Rev. B **50**, 7398 (1994).
[8] M. L. Cohen and T. K. Bergstresser, Phys. Rev. **141**, 789 (1966).
[9] M. L. Cohen and J. R. Chelikowski, *Electronic Structure and Optical Properties of Semiconductors* (Springer, Berlin, 1988), p. 142.
[10] D. B. Laks, G. F. Neumark, A. Hangleiter, and S. T. Pantelides, Phys. Rev. Lett. **61**, 1229 (1988).
[11] Z. H. Levine and S. G. Louie, Phys. Rev. B **25**, 6310 (1982); see also M. S. Hybertson and S. G. Louie, Phys. Rev. Lett. **55**, 1418 (1985); Phys. Rev. B **34**, 5390 (1986).
[12] P.-O. Löwdin, J. Chem. Phys. **19**, 1396 (1951).
[13] J. Bude, K. Hess, and G. J. Iafrate, Phys. Rev. B **45**, 10 958 (1992).
[14] L. V. Keldysh, Zh. Eksp. Teor. Fiz. **37**, 713 (1959) [Sov. Phys. JETP **10**, 509 (1960)].
[15] K. Král, Phys. Rev. B **50**, 7988 (1994).
[16] K. Kim, K. Kahen, J. P. Leburton, and K. Hess, J. Appl. Phys. **59**, 2595 (1986).
[17] Y. Kamakura *et al.*, J. Appl. Phys. **75**, 3500 (1994).
[18] K. Brennan, J. Appl. Phys. **64**, 4024 (1988).
[19] S. S. Pennathur, K. Bhattacharyya, J. F. Wager, and S. S. Goodnick, in *Proceedings of the 3rd International Workshop on Computational Electronics*, edited by S. S. Goodnick (Oregon State University Press, Corvallis, 1994), pp. 288–291.